

EUROPHYSICS LETTERS

*Europhys. Lett.*, (), pp. ()

## Fluid-fluid phase separation in hard spheres with a bimodal size distribution

P. B. WARREN

*Unilever Research Port Sunlight Laboratory,  
Quarry Road East, Bebington, Wirral, L63 3JW, UK.*

(received ; accepted )

PACS. 05.20-y – Statistical mechanics.

PACS. 64.75+g – Solubility, segregation and mixing.

PACS. 82.70Dd – Colloids.

**Abstract.** – The effect of polydispersity on the phase behaviour of hard spheres is examined using a moment projection method. It is found that the Boublik-Mansoori-Carnahan-Starling-Leland equation of state shows a spinodal instability for a bimodal distribution if the large spheres are sufficiently polydisperse, and if there is sufficient disparity in mean size between the small and large spheres. The spinodal instability direction points to the appearance of a very dense phase of large spheres.

The phase behaviour of hard sphere mixtures has received much attention recently following the observation by Biben and Hansen [1] that, with an improved closure approximation, integral equation theory indicates the presence of a fluid-fluid spinodal instability in a bidisperse mixture if the ratio of the large to small sphere diameters is  $\gtrsim 5$ . Several experimental groups report confirmatory evidence [2, 3, 4]. The dense phase of the large spheres is sometimes observed to be an ordered phase and at other times to be an amorphous colloidal glass, although some discrepancies in detail remain [3, 4].

Numerical solutions to integral equations frequently only suggest the existence of a spinodal instability, from the apparent divergence of the structure factor for instance. Thus for binary hard spheres, Caccamo and Pellicane [5] can argue that the integral equation evidence supports fluid-solid segregation rather than fluid-fluid separation. Recent computer simulations support this scenario, by establishing that a region of fluid-fluid coexistence exists, but is metastable with respect to fluid-solid coexistence [6].

Analytic solutions to integral equations, although rare and generally perceived to be less accurate than numerical solutions, do not suffer from the same problems. Most notable of these for hard spheres is the Percus-Yevick closure [7]. As reported by Lebowitz and Rowlinson [8] though, this closure predicts that a binary hard sphere fluid is stable for all size ratios and physically accessible compositions.

The appeal of the Percus-Yevick approximation is tempered by an internal inconsistency between the compressibility equation of state (EOS) and the virial EOS. It is precisely this

inconsistency that the new closure approximations mentioned above are designed to cure. A phenomenological way around this problem though is to interpolate between the two EOS's. For monodisperse hard spheres, a suitable interpolation leads to the highly successful Carnahan and Starling EOS [9]. For an arbitrary mixture, the same interpolation leads to an EOS first considered by Boublik and Mansoori *et al* (BMCSL EOS) [10]. This improved EOS also predicts phase stability for a binary hard sphere fluid for any size ratio and composition.

It is well known though that polydispersity enhances phase instability. An interesting and experimentally relevant question therefore concerns the effects of size polydispersity on the phase behaviour of hard sphere mixtures. Fortunately the above EOS's have been extended to polydisperse systems, for instance the Helmholtz free energy and related thermodynamic quantities corresponding to the BMCSL EOS are given by Salacuse and Stell [11] in terms of the number density and the first three moments of the size distribution.

For the Percus-Yevick compressibility EOS, Vrij [12] established that an arbitrarily polydisperse hard sphere fluid is stable, thus confirming a conjecture of Lebowitz and Rowlinson [8]. However the question of whether, under the BMCSL EOS, a binary mixture becomes unstable if one or both of the species is allowed to become polydisperse has not to my knowledge been previously investigated. Perhaps surprisingly in the light of Vrij's result the answer to this question is "yes". Moreover the instability reflects the experimental observations, albeit at a much larger degree of polydispersity and size ratio than are seen in reality. Very recently Cuesta has found a similar spinodal instability in hard spheres with a unimodal, log-normal size distribution [13].

I address the spinodal stability problem using a novel moment projection method developed recently by Sollich and Cates [14] and myself [15]. The approach reduces the free energy to one which depends only on moment densities (defined below). It gives exact results for cloud and shadow curves (the polydisperse analogues of the binodal) and for spinodal curves, provided the excess free energy is a function only of the corresponding moments of the size distribution. Since the BMCSL excess free energy is precisely of this form, the new tool may be applied to this situation. By way of contrast, Cuesta approaches the spinodal problem by casting it as an integral equation [13]. He also finds that if the excess free energy depends only on a few moments, the integral equation is reducible to a matrix problem, which can in fact be proved to be identical to the results obtained below. Such a reduction in dimensionality for the spinodal problem has been noted several times in the past [16].

I outline the approach in general first to indicate its application to spinodal curves, which was not previously covered in detail. Suppose that the excess free energy depends only on a few moment densities, defined to be  $\phi_n = \sum_{i=1}^N f_n(\sigma_i)/V$ , where  $V$  is the system volume and the functions  $f_n(\sigma)$  are arbitrary. The sum is over all particles in a homogeneous phase, and the  $\sigma_i$  are individual particle properties, such as size. If we set  $f_0(\sigma) = 1$  then we include the number density  $\rho = \phi_0$  amongst the moment densities (in doing this though the  $n = 0$  term should be omitted from certain sums below). As previously reported, moment densities can be treated as independent thermodynamic density variables provided the ideal part of the free energy density is suitably generalised:

$$f^{(\text{id})} = \rho k_B T (\ln \rho - 1) - \rho T s(m_n) \quad (1)$$

where  $s(m_n)$  is a generalised entropy of mixing per particle, and  $m_n = \phi_n/\rho = \sum_{i=1}^N f_n(\sigma_i)/N$  ( $n > 0$ ) are generalised moments. An expression for  $s(m_n)$  can be given only if the parent or feedstock distribution,  $p(\sigma)$ , is specified. This is because one must know the parent distribution from which particles are drawn, to conclude anything about the distributions in daughter phases. The generalised entropy of mixing is then given by a Legendre transform (I will set

$k_B = T = 1$  in the following for simplicity):

$$s(m_n) = h(\theta_n) + \sum_{n>0} \theta_n m_n, \quad m_n = -\frac{\partial h}{\partial \theta_n}, \quad (2)$$

where the function  $h$  is a generalised cumulant generating function for  $p(\sigma)$ ,

$$h = \ln \int d\sigma p(\sigma) \exp \left[ - \sum_{n>0} \theta_n f_n(\sigma) \right]. \quad (3)$$

The excess free energy density,  $f^{(\text{ex})}(\phi_n)$ , is added to  $f^{(\text{id})}$  to obtain the overall free energy density  $f$ . The spinodal stability condition is then the standard one of positive definiteness of the matrix of second partial derivatives of  $f$  with respect to the  $\phi_n$  (including  $\phi_0 = \rho$  amongst these). For the ideal part these second derivatives are readily shown to be

$$\begin{aligned} \frac{\partial^2 f^{(\text{id})}}{\partial \phi_0^2} &= \frac{1}{\rho} - \frac{1}{\rho} \sum_{n,r>0} m_n m_r \frac{\partial^2 s}{\partial m_n \partial m_r}, & \frac{\partial^2 f^{(\text{id})}}{\partial \phi_0 \partial \phi_n} &= \frac{1}{\rho} \sum_{r>0} m_r \frac{\partial^2 s}{\partial m_n \partial m_r}, \quad (n > 0), \\ \frac{\partial^2 f^{(\text{id})}}{\partial \phi_n \partial \phi_r} &= -\frac{1}{\rho} \frac{\partial^2 s}{\partial m_n \partial m_r}, \quad (n, r > 0). \end{aligned} \quad (4)$$

The key is clearly the matrix  $\partial^2 s / \partial m_n \partial m_r$ . It can be easily shown from eq. (2) that if  $(\mathbf{A})_{nr} = \partial^2 h / \partial \theta_n \partial \theta_r$  ( $n, r > 0$ ), then  $\partial^2 s / \partial m_n \partial m_r = -(\mathbf{A}^{-1})_{nr}$ .

Since the parent distribution enters into the solution in an essential way, it constrains the mean values of the moments to those of the parent distribution. This constraint is essential to obtain the exact spinodal and related stability conditions, and cloud and shadow curves. For a homogeneous system, it means that after all calculations have been completed the results should be constrained to lie on the physical dilution line,  $\phi_n / \rho = m_n = \langle f_n(\sigma) \rangle_p$  where  $\langle \dots \rangle_p = \int d\sigma p(\sigma) (\dots)$ . Fortunately this constraint has a simple implementation. By explicit differentiation of eq. (3) the moments are given as functions of  $\theta_n$  by

$$m_n = e^{-h} \int d\sigma p(\sigma) f_n(\sigma) \exp \left[ - \sum_{r>0} \theta_r f_r(\sigma) \right]. \quad (5)$$

Since the map  $\theta_n \leftrightarrow m_n$  should be 1 : 1, otherwise the Legendre transform is ill defined, the dilution line constraint is seen to correspond to the point  $\theta_n = 0$ . This observation now makes it obvious why stability conditions such as the spinodal condition, the critical point, and so on depend only on a finite set of moments or cumulants of the parent distribution. These conditions involve second or higher order derivatives of  $h$  evaluated on the dilution line, which corresponds to the point  $\theta_n = 0$ . Since  $h$  is a cumulant generating function, these derivatives are precisely the cumulants of  $p(\sigma)$ . This observation generalises a number of moment truncation theorems reported previously by other workers [16]. Applying this dilution line constraint to the matrix  $\mathbf{A}$  obtains for instance

$$(\mathbf{A})_{nr} = \langle f_n(\sigma) f_r(\sigma) \rangle_p - \langle f_n(\sigma) \rangle_p \langle f_r(\sigma) \rangle_p. \quad (6)$$

This matrix is readily inverted for use in eqs. (4).

The spinodal stability limit corresponds to a vanishing eigenvalue of the matrix of second partial derivatives of the free energy. The associated eigenvector contains valuable but oft-neglected information on the spinodal instability direction. This is the direction in composition space in which the homogeneous system starts to become unstable towards small perturbations, as the spinodal line is crossed. It can be used to determine (mean-field) critical points, as

points where the instability direction is tangent to the spinodal line. Away from such points, the instability direction tends to reflect the slope of tielines connecting coexisting phases.

In the Sollich-Cates picture [14], the spinodal instability is contained in the family of size distributions  $p(\sigma)\exp[\sum\lambda_n f_n(\sigma)]$ . Expanding this about a point on the dilution line indicates that, in terms of a size distribution, the spinodal instability direction is contained in  $\Delta\rho(\sigma) = \rho p(\sigma)\sum\Delta\lambda_n f_n(\sigma)$ , where the prefactor  $\rho$  comes from the  $n = 0$  term. The  $\Delta\lambda_n$  can be found from the constraints  $\int d\sigma f_n(\sigma)\Delta\rho(\sigma) = \Delta\phi_n$  where  $\Delta\phi_n$  is the prescribed eigenvector. From this, if  $(\mathbf{B})_{nr} = \langle f_n(\sigma)f_r(\sigma) \rangle_p$  ( $n, r \geq 0$ ), the spinodal instability direction is

$$\Delta\rho(\sigma) = p(\sigma) \sum_{n,r \geq 0} f_n(\sigma)(\mathbf{B}^{-1})_{nr}\Delta\phi_r. \quad (7)$$

Actually, in the Sollich-Cates picture one can also show that the matrix  $\partial^2 f^{(\text{id})}/\partial\phi_n\partial\phi_r = ((\rho\mathbf{B})^{-1})_{nr}$  [17]. The equivalence to eqs. (4) can be established with some algebra. Note that if the  $f_n(\sigma)$  ( $n \geq 0$ ) form an orthonormal set with  $p(\sigma)$  as a weight function, the matrices  $\mathbf{A}$  and  $\mathbf{B}$  become unit matrices, and many of these results simplify markedly.

I now apply this machinery to examine the spinodal stability of hard spheres. It is convenient to introduce a fiducial diameter  $\sigma_0$  and scale all densities with  $\pi\sigma_0^3/6$ . The excess free energy density corresponding to the BMCSL EOS is given by Salacuse and Stell [11]

$$\frac{\pi\sigma_0^3}{6} f^{(\text{ex})} = \left(\frac{\phi_2^3}{\phi_3^2} - \phi_0\right) \ln(1 - \phi_3) + \frac{3\phi_1\phi_2}{1 - \phi_3} + \frac{\phi_2^3}{\phi_3(1 - \phi_3)^2}. \quad (8)$$

The moment densities are  $\phi_n = (\pi\sigma_0^3/6)\rho m_n$  and the moment functions themselves are  $f_n(\sigma) = (\sigma/\sigma_0)^n$ . Thus  $\phi_0 = \pi\sigma_0^3\rho/6$  is now a dimensionless number density, and  $\phi_3 = \phi$  is the volume fraction.

For the parent distribution I take either a Schulz distribution with an extra monodisperse component or a mixture of two Schulz distributions. I will characterise these by the mean diameter and the degree of polydispersity, where the latter is the ratio of the standard deviation to the mean diameter (usually expressed as a percentage). The moments  $\langle(\sigma/\sigma_0)^n\rangle_p$  which appear in the matrices  $\mathbf{A}$  and  $\mathbf{B}$  are given by simple algebraic relations once the distributions have been specified.

The  $4 \times 4$  spinodal determinant is constructed as described above, and examined as a function of the ratio of mean diameters,  $\sigma_L/\sigma_S$ , the degree of polydispersity of the two components,  $\delta_L$  and  $\delta_S$ , and the volume fractions of the two components,  $\phi_L$  and  $\phi_S$ . Generally the determinant is always positive except when a large value of the diameter ratio,  $\sigma_L/\sigma_S \gtrsim 60$ , is combined with a large degree of polydispersity of the large spheres,  $\delta_L \gtrsim 50\%$ .

Fig. 1(a) shows the spinodal instability appearing as the diameter ratio is increased, for a bimodal distribution with a monodisperse small component. Fig. 1(b) shows the same for fixed mean diameter ratio and increasing degree of polydispersity of both components. Interestingly, at fixed mean diameter ratio and degree of polydispersity of the large component, the instability region diminishes as the degree of polydispersity of the small species increases. This is illustrated in fig. 2. In both figures, results are only shown for the physically reasonable region  $\phi_S + \phi_L \lesssim 0.5$ .

The tick marks (short lines) on the spinodal lines indicate the spinodal instability direction projected into the  $(\phi_S, \phi_L)$  plane. The insets to these figures show unnormalised parent distributions at one selected point in each plot together with the spinodal instability direction from eq. (7). Thus in fig. 1(b) for example, at the marked point, the system is unstable towards a composition fluctuation in which the density of large spheres increases and the

density of small spheres decreases: the precise functional form of the composition fluctuation is the dashed line in the inset.

The tick marks and insets show that the instability is one of demixing with some additional size partitioning. The instability direction, as indicated by the tick marks for instance, is never found to be tangential to the spinodal line in the physical region although it does approach this condition for high values of the large sphere volume fraction. This clearly points to a critical point lying at large  $\phi_L$  and suggests that the equilibrium state is one of a highly dense fluid of large spheres coexisting with much less dense fluid of mostly small spheres. Note that the degree of polydispersity for the large spheres is easily large enough to suppress the formation of an ordered phase [18].

Why should polydispersity have this effect? If one introduces small spheres into a fluid of large spheres, depletion forces in the latter are apparently insufficient to bring about phase separation, at least according to the BMCSL EOS. It is known though that polydispersity decreases the pressure of a hard sphere fluid [10], due to relaxed packing constraints. It appears from the present calculation that polydispersity can make the large sphere fluid sufficiently compressible for the small sphere depletion forces to induce fluid-fluid phase separation. What is remarkable is that the BMCSL EOS appears to capture this effect, without being specifically designed to do so.

These results show intriguing parallels with the experimental observations, with regard to the nature of phase separation in hard sphere mixtures. In the experiments [2, 3, 4], phase separation is observed at a much smaller diameter ratio, typically  $\sigma_L/\sigma_S \sim 10$ , and degree of polydispersity, typically  $\lesssim 10\%$ . The dense phase of large spheres is also observed to be crystalline or amorphous. These differences are presumably due to the sensitivity of the phase boundary to the accuracy of the EOS, as reported by Biben and Hansen [1] (given this sensitivity, one can speculate whether the discrepancies between experimental results [3, 4] for size ratio dependence may be due to polydispersity effects). Also, if the polydispersity in the dense phase is sufficiently small, ordering into a crystal phase is likely to take place. The novelty of the present analysis is that the broad picture is reproduced by the BMCSL EOS, if polydispersity is taken into account.

Some intriguing possibilities still remain though for the true equilibrium phase diagram of an arbitrarily polydisperse mixture. One such is fractionation into multiple crystalline phases [19]. Another is to relax the packing constraints in a dense crystal by degrading the crystal symmetry from FCC, or the formation of superlattice structures which could be regarded as interpenetrating multiple crystals. At high volume fractions though, the glass transition and other kinetic considerations undoubtedly play a major role in determining what is observed experimentally.

\*\*\*

I acknowledge useful correspondence with JOSÉ CUESTA, RICHARD SEAR and PETER SOLLICH.

## REFERENCES

- [1] BIBEN T. and HANSEN J. P., *Phys. Rev. Lett.*, **66** (1991) 2215.
- [2] SANYAL S., EASWAR N., RAMASWAMY S. and SOOD A. K., *Europhys. Lett.*, **18** (1992) 107; VAN DUJNEVELDT J. S., HEINEN A. W. and LEKKERKERKER H. N. W., *Europhys. Lett.*, **21** (1993) 369; KAPLAN P. D., ROUKE J. L., YODH A. G. and PINE D. J., *Phys. Rev. Lett.*, **72** (1994) 582; IMHOF A. and DHONT J. K. G., *Phys. Rev. Lett.*, **75** (1995) 1662.
- [3] STEINER U., MELLER A. and STAVANS J., *Phys. Rev. Lett.*, **74** (1995) 4750.
- [4] DINSMORE A. D., YODH A. G. and PINE D. J., *Phys. Rev. E*, **52** (1995) 4045.

- [5] CACCAMO C. and PELLICANE G., *Physica A*, **235** (1997) 149.
- [6] DIJKSTRA M., VAN ROIJ R. and EVANS R., *Phys. Rev. Lett.*, **81** (1998) 2268.
- [7] LEBOWITZ J. L., *Phys. Rev.*, **133** (1964) A895
- [8] LEBOWITZ J. L. and ROWLINSON J. S., *J. Chem. Phys.*, **41** (1964) 133.
- [9] CARNAHAN N. F. and STARLING K. E., *J. Chem. Phys.*, **51** (1969) 635.
- [10] BOUBLIK T., *J. Chem. Phys.*, **53** (1970) 471; MANSOORI G. A., CARNAHAN N. F., STARLING K. E. and LELAND, JR. T. W., *J. Chem. Phys.*, **54** (1971) 1523.
- [11] SALACUSE J. J. and STELL G., *J. Chem. Phys.*, **77** (1982) 3714.
- [12] VRIJ A., *J. Chem. Phys.*, **69** (1978) 1742.
- [13] CUESTA J. A., cond-mat/9807030 Preprint, 1998.
- [14] SOLLICH P. and CATES M. E., *Phys. Rev. Lett.*, **80** (1998) 1365.
- [15] WARREN P. B., *Phys. Rev. Lett.*, **80** (1998) 1369.
- [16] IRVINE P. and GORDON M., *Proc. R. Soc. Lond. A*, **375** (1981) 397; BEERBAUM S., BERGMANN J., KEHLEN H. and RÄTZSCH M. T., *Proc. R. Soc. Lond. A*, **406** (1986) 63; **414** (1987) 103; HENDRIKS E. M., *Ind. Eng. Chem. Res.*, **27** (1988) 1728.
- [17] SOLLICH P., private communication.
- [18] See, e.g., BARTLETT P., *J. Chem. Phys.*, **107** (1997) 188.
- [19] PUSEY P. N., *J. Physique Lett.*, **48** (1987) 709; BARTLETT P., *J. Chem. Phys.*, **109** (1998) 10970; SEAR R. P., *Europhys. Lett.*, **44** (1998) 531.

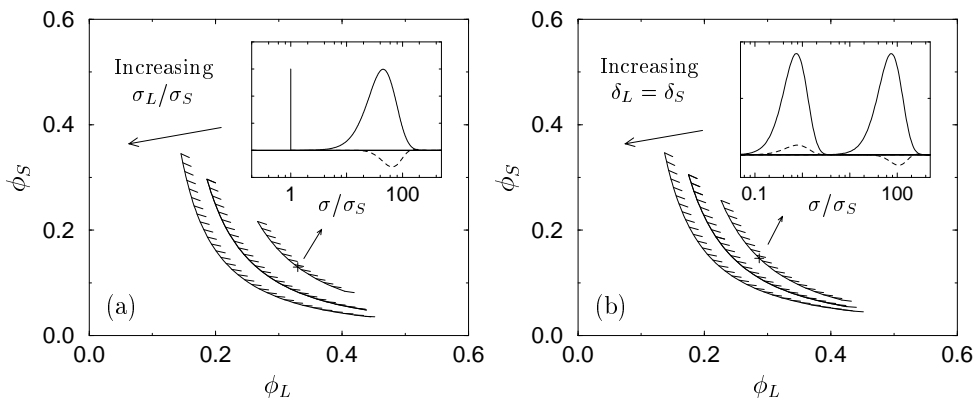


Fig. 1. – Spinodal instability lines for polydisperse hard sphere mixtures (solid lines with tick marks in main plots): (a) monodisperse small spheres mixed with polydisperse large spheres,  $\delta_L = 50\%$ , for  $\sigma_L/\sigma_S = 60, 80$  and  $100$ , and (b) mixture of polydisperse small and large spheres at  $\sigma_L/\sigma_S = 100$ , for  $\delta_L = \delta_S = 50\%, 65\%$  and  $90\%$ . The tick marks indicate the spinodal instability direction. The insets show the (unnormalised) size distribution (solid lines) and the direction in which it is spinodally unstable (dotted lines), at the marked points.

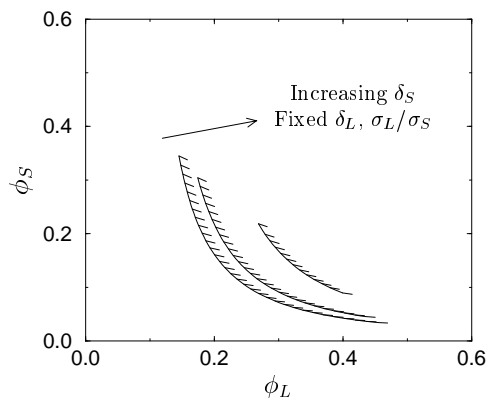


Fig. 2. – Mixture of polydisperse small and large spheres at  $\sigma_L/\sigma_S = 100$ ,  $\delta_L = 50\%$ , for  $\delta_S = 0$  (monodisperse),  $30\%$  and  $60\%$ .